J Solid State Electrochem (2009) 13:639–649
DOI 10.1007/s10008-008-0639-7

ORIGINAL PAPER

The overall adhesion-spreading process of liposomes on a mercury electrode is controlled by a mixed diffusion and reaction kinetics mechanism

Víctor Agmo Hernández · Michael Hermes · Alexander Milchev · Fritz Scholz

Received: 30 June 2008 / Revised: 24 July 2008 / Accepted: 28 July 2008 / Published online: 29 August 2008

Abstract Using high-resolution chronoamperometric measurements, with sampling each 1.333 μs, the initial step of the adhesion-spreading of liposomes on a mercury electrode was studied. These measurements allow getting a deeper insight into the first interaction of the liposomes with the mercury electrode, and they show that the overall adhesion-spreading process at different potentials is partially controlled by a fast but weak interaction equilibrium resulting in a mixed diffusion- and reaction-kinetics-controlled mechanism of the overall reaction.

Keywords Liposomes · Chronoamperometry · Adhesion-spreading · Mercury electrode · DMPC

The authors dedicate this contribution to Keith Oldham on the occasion of his 80th birthday. Since my (FS) first meeting with Keith Oldham in Alan Bond's laboratory in Australia in 1987, I had the privilege to get Keith's unerring advice and have stimulating discussions with him for which I like to cordially thank him.

M. Hermes · F. Scholz (✉)
Institut für Biochemie, Universität Greifswald,
Felix-Hausdorff-Str. 4,
17487 Greifswald, Germany
e-mail: fscholz@uni-greifswald.de

A. Milchev
Rostislaw Kaischew Institute of Physical Chemistry,
Bulgarian Academy of Sciences,
Acad. G. Bonchev Str. bl. 11,
1113 Sofia, Bulgaria

Present address:
V. Agmo Hernández
Department of Physical and Analytical Chemistry,
Division of Physical Chemistry, Uppsala University,
Box 579, 751 23 Uppsala, Sweden

Introduction

The study of the fundamental properties of lipid self-assembled structures, especially lipid membranes, has been shown to be of great importance in order to design vesicles and other membrane structures which mimic real cell biomembranes and allow the development of novel drug delivery systems [1–8]. The details of the adhesion-spreading of liposomes on a static mercury drop electrode can be unraveled by applying chronoamperometry [9, 10] because the liposomes lead to the formation of islands of adsorbed lecithin molecules (in the form of a lipid monolayer, as shown by others [11–15]), a process accompanied by changes of the double-layer capacitance producing capacitive current spikes (peaks) in the chronoamperometric traces [9, 10, 16–18]. Each spike represents the adhesion-spreading of a single liposome, and therefore the adhesion-spreading can be studied individually for each vesicle. The sign of the peak current depends on the sign of the charge at the electrode surface. At negatively charged electrodes, the decrease in the double-layer capacity caused by liposome adhesion-spreading will generate positive capacitive currents (and therefore positive spikes), while negative peaks will be recorded at positively charged electrodes. The capacitive peaks can be integrated, and the resulting charge transient can be very well fitted to the empirical equation:

$$Q_{\mathrm{lip}}(t) = Q(0) + Q_1(1 - \exp(-t/\tau_1)) + Q_2(1 - \exp(-t/\tau_2)) \quad (1)$$

where $Q_{\mathrm{lip}}(t)$ is the amount of charge displaced due to the liposome adhesion-spreading as a function of time. Three contributions can be distinguished: (a) A very fast "docking" step (using the nomenclature of Hellberg et al. [10]),

the time constant of which was until now not accessible due to a too low resolution of the performed measurements; (b) an "opening" step with the time constant τ_1 during which the bilayer structure of the membrane is perturbed as the outer lecithin molecules must turn around in order to expose their lipophilic ends to the hydrophobic mercury surface; and finally (c) a "spreading" step with the time constant τ_2 during which an open pore is formed in the membrane, causing its rupture and spreading and leading to the formation of an adsorbed lecithin island. Besides the high correlation between Eq. 1 and the experimentally obtained data, the model is supported also by a theoretical model [10]. That adhesion-spreading model is further backed by other experimental results [16–18]. The goodness of the fit and the accuracy of Eq. 1 were evaluated quantitatively estimating the chi-square-based probability Q as described in [19], demonstrating that the good correlation between the model and the experimental curves is not trivial. However, it turned out that the nomenclature for designating the process steps needs a revision. Therefore, we propose instead of the abovementioned terms the following terms: (a) interaction-docking, (b) bilayer opening, and (c) rupture-spreading, and these will be used in the present paper.

Our adhesion-spreading model resembles the widely accepted mechanism of membrane fusion consisting also of three steps: contact making, hemifusion, and fusion [20–26]. These processes correspond to our model in the following way: (a) interaction-docking ⇔ first contact making; (b) bilayer opening ⇔ hemifusion stalk formation, (c) and rupture-spreading ⇔ fusion pore formation.

Determining the time constants and activation energies of the processes, the effect of liposome lamellarity, temperature, phase composition, and of embedded molecules (other lipids or peptides) on the general properties of the membrane (resistance to rupture, bending rigidity, activation energy for flip-flop translocation, phase transition temperature (PTT), etc.) can be estimated [16–18].

This model, as well as the interpretation of the spike shaped signals, has been criticized before, and an alternative model of adhesion-spreading of liposomes on mercury has been proposed [27]. However, these authors assume the formation of a lipid bilayer on the mercury surface, which is in clear contradiction to previous studies [11–15]. Furthermore, the three-step adhesion-spreading model developed by the Greifswald group provides a consistent explanation of signals observed for liposomes with different compositions and under different conditions [28], whereas the challenging model only explains the observations made with one kind of liposomes and under very specific experimental conditions. The latter observations can also be explained by the three-step adhesion model, considering the kind of liposomes that were used.

It has been shown before that high-resolution chronoamperometric measurements are an excellent tool to characterize the interaction of electrodes with different kinds of particles [29–34]. In the present communication, we report about the use of high-resolution measurements in order to determine the time dependence of the interaction-docking step (first term on the right side of Eq. 1) and about its implications for the overall adhesion-spreading mechanism of liposomes on a mercury electrode.

Experimental

High-purity 1,2-dimyristoyl-*sn*-glycero-3-phosphocholine (DMPC; Lipoid GmbH, Ludwigshafen, Germany) was used without further purification. KCl (Suprapur®; Merck, Darmstadt, Germany) and Millipore water were used for all solutions and liposome suspensions. Before measuring, the suspensions were deaerated for 20 min with high-purity nitrogen. Electrochemical measurements were performed with an AUTOLAB PGSTAT 12 (Eco Chemie, Utrecht, The Netherlands) with an ACD164 modulus interfaced to a P4 PC in conjunction with an electrode stand VA 663 (Metrohm, Herisau, Switzerland). The electrochemical measuring device has a rising time of 500 ns. A multimode mercury electrode was used as working electrode, a platinum rod served as auxiliary electrode, and an Ag|AgCl (3 M KCl, E=0.208 V vs. standard hydrogen electrode) electrode was used as reference electrode. The surface area of the mercury drop was 0.48 mm^2, as determined by weighting 50 drops. The high-resolution chronoamperometric measurements were performed within 40 ms with sampling each 1.333 μs at potentials between −0.1 and −0.9 V vs. Ag|AgCl in 100 mV steps, following a 1 s conditioning step. For the determination of the number of adhesion signals as a function of the elapsed time, 50 low-resolution measurements (within 1.5 s and with sampling each 50 μs) were performed in the same potential range at 25 °C, and the average number of peaks in the elapsed time was determined in 1.5 ms steps. The program "Signal Counter" [35] was used to determine the number of obtained peaks. The solutions were thermostated with an accuracy of ±0.1 K.

Giant unilamellar vesicles (GUVs) were prepared according to Moscho et al. [36]. Three milligrams of DMPC were dissolved in 2.2 mL of a 1:10 methanol/chloroform mixture. Then, 30 mL of 0.1 M KCl solution was added carefully by pouring along the flask walls, following to which the organic solvent was rapidly removed with the help of a rotary evaporator (Laborota 4000, Heidolph, Nürnberg, Germany) using a Rotavac control pump (Heidolph) at 40 °C and a final pressure of 10 mbar. The rotation speed was 30 rpm. This way, a clear

suspension containing a high yield of GUVs could be obtained. The formation of GUVs was confirmed by comparing the size distribution obtained by light scattering with the size distribution of the chronoamperometric peaks, which changes according to the lamellarity [10, 16]. Temperature variation experiments (with 3 K steps) were performed by slowly cooling down the freshly prepared liposomes. After reaching the PTT (23.5 °C), the suspension was cooled to 2 °C, and the temperature was then slowly risen to the pretransition temperature (11 °C) and then slowly increased in 3-K increments, performing high-resolution measurements until recording an average of ten adhesion signals for each temperature. This temperature program had the objective to minimize shape changes [37, 38], especially when the lecithin was in the liquid crystalline phase, and to be able to generate the pretransition rippled gel phase.

Results and discussion

Microscopical approach to the interaction-docking step and the overall kinetics

To analyze the time dependence of the interaction-docking step, i.e., the first contact making between a liposome and the electrode surface, it is necessary to consider the time dependence of the first right-hand term in Eq. 1. We probed the simple assumption that this process may also follow first-order kinetics, similar to the two follow-up steps. Hence, we substituted the time-independent term $Q(0)$ in Eq. 1 (which assumes an instant docking) by the first-order expression $Q_0(1-\exp(-t/\tau_0))$ introducing the time constant τ_0 to describe the interaction-docking process as a function of time and expanding Eq. 1 as follows:

$$Q_{\mathrm{lip}}(t) = Q_0(1-\exp(-t/\tau_0)) + Q_1(1-\exp(-t/\tau_1)) + Q_2(1-\exp(-t/\tau_2)) \quad (2)$$

Using high-resolution measurements, it is possible to sample a sufficient number of experimental data points at the beginning of the adhesion-spreading process to determine τ_0. Figure 1 shows a typical high-resolution chronoamperometric signal demonstrating two liposome adhesion-spreading events. In the depicted case, the background noise amplitude is rather large, but it can be considerably reduced by a fast Fourier transform (FFT) filter which removes all Fourier components with frequencies above 50 kHz. Such smoothing was not always necessary, as the amplitude of the background noise was highly dependent on the environmental conditions and could be in some cases reduced to only 1 nA. The results derived from smoothed curves and from direct experimental curves did not show any significant difference. Taking just the larger peak shown in Fig. 1, it is possible to analyze the adhesion-spreading event of just the vesicle generating that signal. Figure 2 shows the isolated peak after smoothing and the charge transient obtained by integration of the peak. By fitting the curve in Fig. 2b with both Eqs. 1 and 2, it was obvious that both models are suitable; however, Eq. 2 predicts much better the behavior during the first microseconds of the adhesion-spreading process (cf. Fig. 3). This improvement results from the fact that the initial interaction-docking process is not considered instantaneous as in the previous model, therefore satisfying the experimental observed condition of $Q_{\mathrm{lip}}(0)=0$. Depending on the temperature, the time constant τ_0 of interaction docking for DMPC GUVs under the conditions described in "Experimental" is between 1 and 15 μs. Of course, it was impossible to analyze the time dependence of Q_0 with the 50 μs resolution used in previous experiments.

By determining τ_0 at different temperatures, the activation energy of the interaction-docking process is accessible by performing an Arrhenius analysis. As follows from Fig. 4, the activation energy of the process is independent of the nature of the DMPC phase of the liposomes (i.e., whether it is in the gel or liquid crystalline phase), since the Arrhenius plot does not change its slope at the phase transition temperature (PTT=23.5 °C for DMPC). In previous publications [10, 16], it has been shown that a similar continuity is observed at the PTT for the overall adhesion-spreading kinetics (defined as the frequency of recorded adhesion-spreading events), although not for the two microscopical processes bilayer opening and rupture-spreading. This observation indicates that the overall process (frequency of adhesion events) is controlled at the

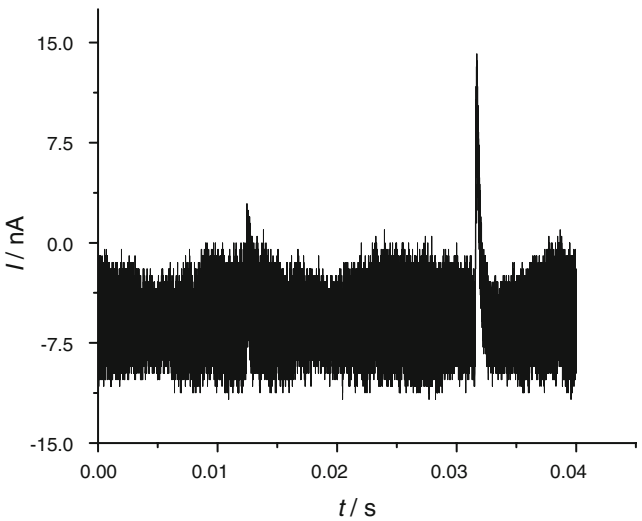

Fig. 1 High-resolution chronoamperometric signal (without noise reduction by FFT) obtained at −0.9 V vs. Ag|AgCl in a suspension of 0.1 g L^{-1} of DMPC GUVs in 0.1 mol L^{-1} KCl at 35 °C

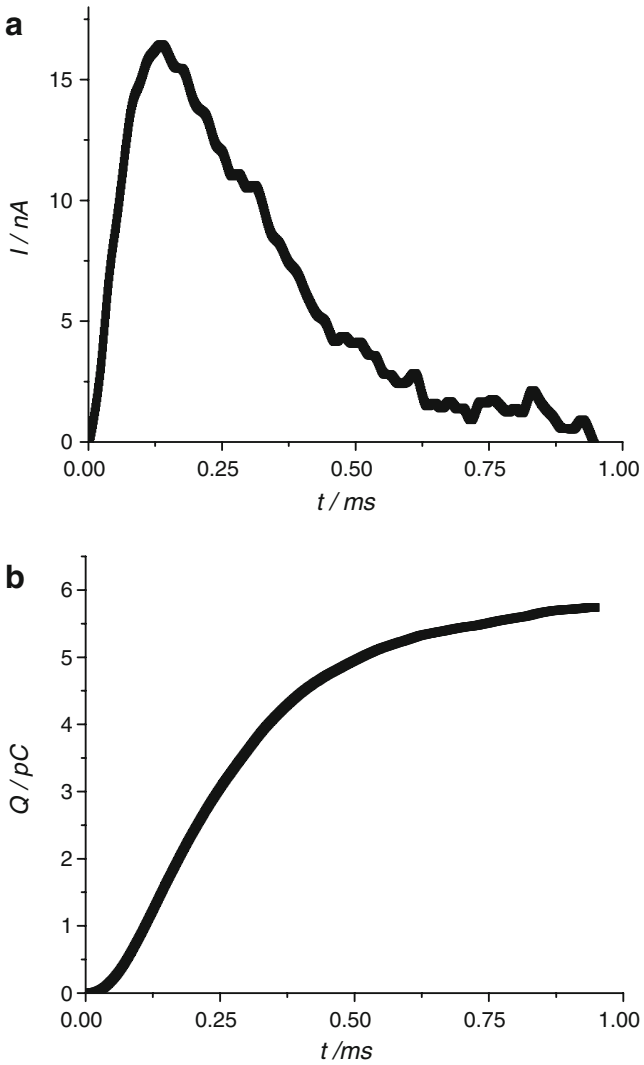

Fig. 2 High-resolution chronoamperometric peak (**a**) and integrated signal (**b**) of a DMPC GUV at 35 °C obtained at a potential of –0.9 V vs. Ag|AgCl

microscopic level mainly by the step described by the time constant τ_0, i.e., the interaction-docking step. This is surprising, given that it is the fastest microscopical process, and one would expect the overall reaction to be controlled by the slowest step, i.e., the rupture-spreading. In order to explain the above-described observations, a theoretical model needs to be developed which accounts for the first-order rate profile introduced in Eq. 2 and for the dependence of the overall adhesion kinetics on the interaction-docking step. This model is a slight modification of the mechanism proposed by Hellberg et al. [10]: a backward reaction (i.e., the reaction of L_D to L′ in the following scheme) is introduced for the interaction-docking step, resulting in the reaction sequence:

$$\mathrm{L} \underset{k_p}{\overset{\text{Trans.}}{\rightleftharpoons}} \mathrm{L'} \underset{k_b}{\overset{k_a}{\rightleftharpoons}} \mathrm{L_D} \underset{\leftarrow}{\overset{\rightarrow}{K_1}} \mathrm{L_{D^*}} \xrightarrow{k_1} \mathrm{L_O} \underset{\leftarrow}{\overset{\rightarrow}{K_2}} \mathrm{L_{O^*}} \xrightarrow{k_2} \mathrm{L_E} \underset{\leftarrow}{\overset{\rightarrow}{K_3}} \mathrm{L_A} \quad (3)$$

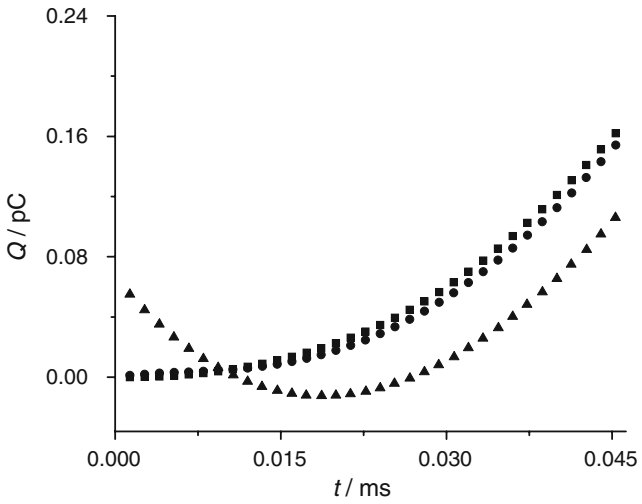

Fig. 3 First microseconds of the integrated transient shown in Fig. 2b. *Squares*: experimental points, *circles*: Fitting with Eq. 2, *triangles*: Fitting with Eq. 1

where L is the free liposome, L′ is the liposome in contact with the mercury surface, L_D is the docked liposome, L_{D^*} is the adsorbed docked liposome in a deformed state, L_O is the opened liposome, L_{O^*} the adsorbed opened liposome, L_E, the "deconvoluted" liposome i.e., lecithin island that is not yet adsorbed, and L_A is the island of adsorbed lecithin molecules. According to the model, K_1, K_2, and K_3 are the equilibrium constants of very fast adsorptions equilibria. The model modification means that the step which had the rate constant k_0 in Hellberg's model [10] and which represented the change from a liposome in contact with the electrode to a docked liposome is substituted by a reversible reaction with the forward and backward rate

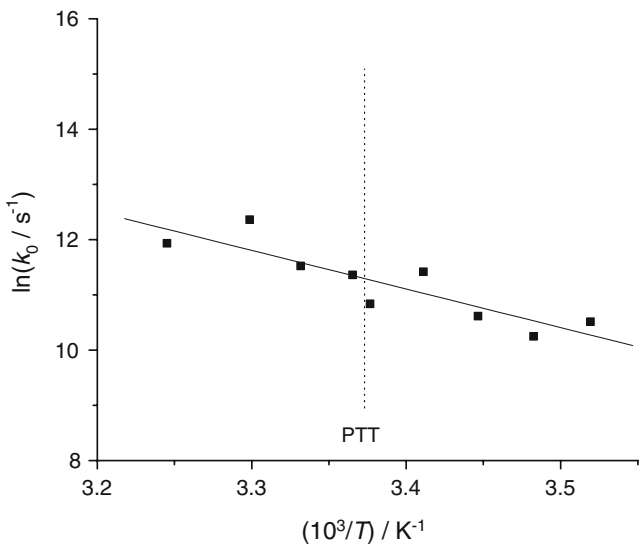

Fig. 4 Arrhenius plot for the interaction-docking of DMPC GUVs calculated from signals obtained at −0.9 V vs. Ag|AgCl. The *solid line* is the linear fitting by the Arrhenius equation

constants k_a and k_b, leaving open the possibility that the first interaction that leads to the docking (interaction-docking step in the expanded model) is reversible. The first reaction represents the transport ("Trans." in Eq. 3) of the liposomes from the bulk to the electrode surface which is also reversible. Solving the appropriate equations (with L′ as the starting point) and expressing the result in terms of the response factor (charge), the following equation is obtained (see Appendix 1):

$$Q_{lip} = Q_0\left(1 - e^{-\frac{t}{\frac{2(1+K_1)}{(Z+Y)}}}\right) + Q_1\left(1 - e^{-\frac{t}{\frac{2(1+K_1)}{(Z-Y)}}}\right) + Q_2\left(1 - e^{-\frac{t}{\frac{(1+K_2)}{(k_2K_2)}}}\right) \quad (4)$$

where

$$Y = \sqrt{(k_b + k_a - k_1K_1 + k_aK_1)^2 + 4K_1k_1k_b}$$
$$Z = k_b + k_a + k_aK_1 + k_1K_1$$

Equation 4 has the same structure like Eq. 2. If $k_a=\infty$ and $k_b=0$, Eq. 4 is reduced to Hellberg's model [10], in which such assumptions were implicitly made (starting point in that model was L_D).

Comparing Eqs. 2 and 4, it follows that:

$$\frac{Z+Y}{2(1+K_1)} = \frac{1}{\tau_0} \quad (5)$$

$$\frac{Z-Y}{2(1+K_1)} = \frac{1}{\tau_1} \quad (6)$$

Further, for k_b and k_a, one obtains:

$$k_a = \frac{1+K_1}{k_1K_1\tau_0\tau_1} \quad (7)$$

$$k_b = -\frac{K_1^2\left(k_1^2\tau_0\tau_1 - k_1(\tau_0+\tau_1)+1\right) + K_1(2 - k_1(\tau_0+\tau_1)) + 1}{k_1K_1\tau_0\tau_1} \quad (8)$$

Note that k_b is positive only for certain values of the involved constants. τ_0 and τ_1 are experimentally accessible, while k_1 can be determined from the low-resolution measurements at low temperatures [10, 16] (below or just above the PTT), leaving K_1 as the only unknown variable, whose value must be adjusted to comply with a positive (or zero) value of k_b. Below, we will show that an approximate value for this constant can be found when considering the overall adhesion-spreading response.

Macroscopical approach

As described in "Experimental," the average number of peaks measured as a function of the elapsed time since the beginning of the experiment was determined in 1.5 ms steps for a suspension of 0.05 g L^{-1} of DMPC GUVs at 25 °C at several potentials. Figure 5 shows the obtained curve at −0.9 V vs. Ag|AgCl. From the time constants already determined for the microscopical process, it is expected that the liposomes already in contact with the electrode undergo adhesion-spreading almost immediately, even if k_b has large values compared with k_a, ruling out pure kinetic control. However, the curve does not correspond neither to pure diffusion control, as the relationship between the number of peaks and the elapsed time does not follow the expected square root relationship. The convective currents that may be caused by the Marangoni effect are unlikely to account for this observation, as they would cause an increase in the number of observed events (as has been reported for the adhesion and spreading of oil droplets and cells on a dropping mercury electrode [39]) instead of a decrease in that parameter on the initial stages as observed here. Therefore, a mixed mechanism is assumed and a complete solution has to take into account all the steps in Eq. 3 up to L_O, where no other possibility is left but the complete adhesion-spreading of the vesicle. However, the system of equations that must be solved for the whole mechanism is very complicated, and a simple solution cannot be found. Therefore, the mechanism was simplified as follows:

$$L \underset{k_p}{\overset{\text{Trans.}}{\rightleftarrows}} L' \underset{k_b}{\overset{k_a}{\rightleftarrows}} L_D \xrightarrow{k_n} N \quad (9)$$

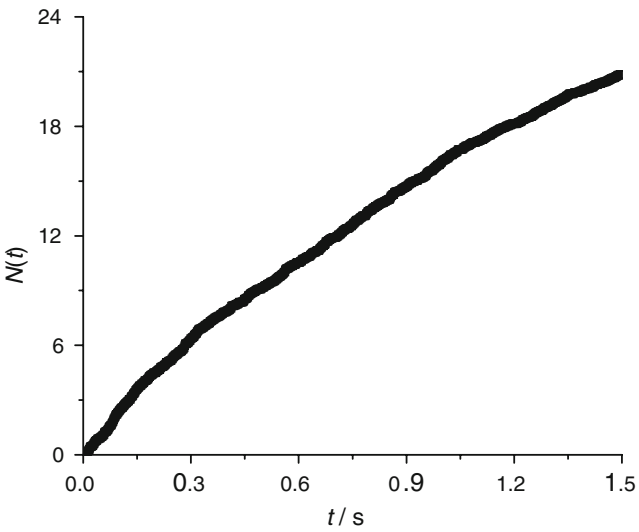

Fig. 5 Average number of observed adhesion-spreading peaks as a function of the elapsed measuring time. Data averaged from 50 measurements on a 0.05-g L^{-1} DMPC GUV suspension in 0.1 M KCl. The *dotted line* is the curve predicted considering diffusion control

where the step with rate constant k_n comprises all steps leading to the irreversible adhesion-spreading. N is the number of recorded adhesion-spreading peaks. In this simplified version, the mechanism going from L′ to N strongly resembles the kinetic equation of metal nucleation on electrodes as proposed by Milchev [40, 41]. In that case, the first reversible step is the formation of active nucleation sites and the second, the actual nucleation of the metal. In our case, the system is analogous; the first step is the "formation" of docked liposomes (forming "nucleation site"), and the second one is the actual "nucleation": an irreversibly attached liposome, which may be either in the L_O, L_E or L_A states. Assuming the transport ("Trans." in Eqs. 3 and 9) to be caused by diffusion, the solution of the pertinent simplified equations (see Appendix 2) leads to:

$$\mathrm{N}(t) = \frac{Z_O \mathrm{erf}\left(\frac{1}{2}\sqrt{t}\sqrt{-2(Y_O+X_O)}\right)}{X_O(Y_O-X_O)(Y_O+X_O)^2\sqrt{-2(Y_O+X_O)}}\exp\left(-\frac{1}{2}(Y_O+X_O)t\right) - \frac{Z_O \mathrm{erf}\left(\frac{1}{2}\sqrt{t}\sqrt{-2(Y_O+X_O)}\right)}{X_O(Y_O-X_O)^2(Y_O+X_O)\sqrt{-2(Y_O-X_O)}} \exp\left(-\frac{1}{2}(Y_O-X_O)t\right) + \frac{2Z_O\sqrt{t}}{\sqrt{\pi}(Y_O-X_O)^2(Y_O+X_O)^2} \tag{10}$$

where:

$$X_O = \sqrt{k_a^2+2k_ak_p+2k_ak_b-2k_ak_n+k_p^2-2k_pk_b-2k_pk_n+k_b^2+2k_nk_b+k_n^2}$$
$$Y_O = k_a+k_p+k_b+k_n$$
$$Z_O = 16A_{SMDE}C_{lip}^*\sqrt{D}k_ak_n\left(k_ak_n+k_pk_b+k_pk_n\right)$$

Simplifying leads to:

$$N(t) = A_{SMDE}C_{lip}^*\sqrt{D} \times \left(A_1\mathrm{erf}\left(\sqrt{-k_{o1}t}\right)e^{-k_{o1}t}+A_2\mathrm{erf}\left(\sqrt{-k_{o2}t}\right)e^{-k_{o2}t}+A_3\sqrt{t}\right) \tag{11}$$

where A_{SMDE} is the area of the electrode, C_{lip}^* is the bulk concentration of the liposomes, and D is the average diffusion coefficient (because there is always a size distribution of liposomes). These three parameters can be determined experimentally: The area of the electrode was determined by weighting the mercury drops, while the average diffusion coefficient and the bulk concentration can be calculated from the size distribution of the liposomes in suspension obtained using light-scattering measurements. The constants A_1 and A_2 have imaginary values that cancel after evaluation of the error functions. Considering together Eqs. 7, 8, and 11, as well as the experimental obtained values of τ_0 and τ_1, and taking into account the fact that k_n is directly related to the values of k_1 estimated for low-resolution measurements, only two unknown constants (K_1 and k_p) are left. Both of them can be obtained by fitting Eq. 11 to the N(t) time dependence curve shown in Fig. 5. Trying several combinations of the values of both constants and calculating k_a and k_b in order to satisfy Eqs. 7 and 8, it was found that the rate constants at the studied temperature and potential must have values on the order of $k_p \approx 0.5\ s^{-1}$, $k_a \approx 10^5\ s^{-1}$, $k_b \approx 10^8\ s^{-1}$, $K_1 \approx 13000$ and $k_n \approx 10^4\ s^{-1}$. It can be seen in Fig. 6 that, using these parameters, the predicted curve corresponds almost perfectly to the experimental one during the first 150 ms of the measuring period in which the standard deviation of the data is small and a diffusion transport mechanism fails completely to describe the process. At longer times, the correspondence is not perfect, but the residual of the model (i.e., the absolute difference between the predicted and the experimental curves) is still much smaller than the standard deviation of the experimental data, as shown in Fig. 7.

Some conclusions can be drawn from the estimated values of the different rate constants. First, the ratio k_a/k_b is very small, around 0.001, meaning that the interaction-docking step, though fast, is very disfavored, and therefore, it controls the overall adhesion-spreading process. This strong tendency of the vesicles *not* to dock on the mercury surface may arise from several reasons: One of them is that the charge density at the electrode surface is quite large, therefore disfavoring the adsorption of suspended particles as has been observed before for other systems [42]. A second reason is that the vesicle fluctuations generate a repulsive force that can be even larger than the attractive van der Waals forces, preventing thus the docking of the vesicles [43, 44]. One could also argue that the attractive adhesion forces are confronted by the increase in bending energy on the vesicle upon adhesion. However, this increase in bending can only prevent the adhesion if the liposomes are small, and in the present case, all liposome

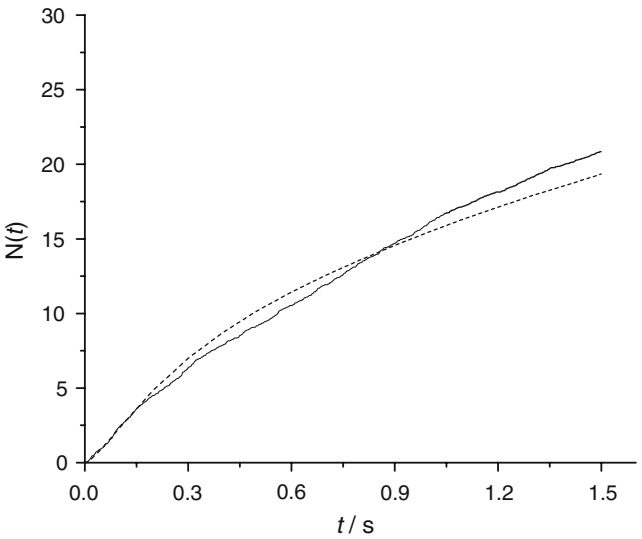

Fig. 6 Number of recorded adhesion events (peaks) as a function of time. *Solid line*: experimental data, *dashed line*: according to the model

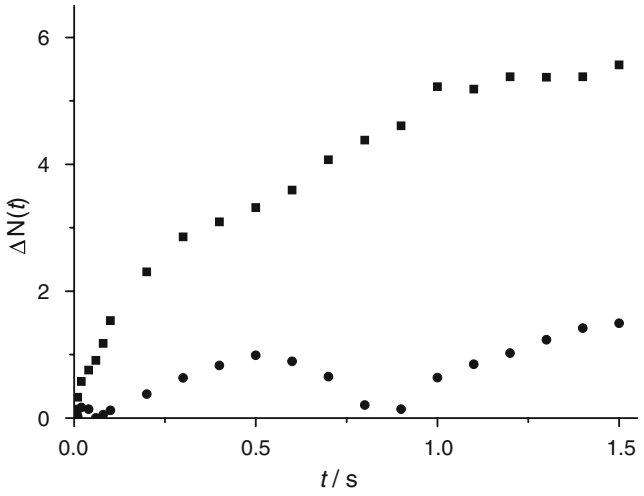

Fig. 7 Experimentally obtained standard deviations of the number of detected liposome adhesion-spreading events as a function of the elapsed time (*squares*) compared with the residuals of the developed theoretical model (*circles*)

adhesion-spreading events studied involve liposomes with a diameter larger than 1 μm, and therefore, they all present a rather large contact area that favors the attractive adhesion interactions [45]. It is also interesting to notice the potential dependence of the constants involved in the overall process, shown in Table 1. It is seen, that at −0.6 V, a potential closer to the point of zero charge (pzc; −0.45 V vs. Ag|AgCl), the interaction-docking step becomes even less favored than at more densely charged electrodes, while the adsorption equilibrium represented by K_1 becomes stronger. The latter observation agrees well with the known behavior of adsorption of organic material at metal electrodes. The reduction in the k_a/k_b, however, suggests that the driving force of the interaction-docking step decreases strongly at potentials near the pzc. A possible explanation is the formation of defects in the bilayer structure when the electric field felt by the membrane is strong, which would happen at large charge densities [15]. The fact that we do not observe anything suggesting the existence of these defects on the resulting adsorbed monolayer can be explained considering that the latter is much more resistant to high electric fields than the liposomes in the suspension [46–48] and that the experiments reported here do not have the sensitivity to detect such defects in the monolayer. The defects of the liposome structure can work as hydrophobic attractive centers [45] and can facilitate the attachment and docking of the liposomes, resulting in the observations reported in the table. In any case, the evidence suggests that the "interaction-docking" step in the model represents the first measurable interaction of the liposome with the electric double layer, which can either result in the adhesion and spreading of the vesicle or more likely—as shown above—the liposome will not undergo the adhesion process.

It is also remarkable that the value of the rate constant k_p is very low compared to all other rate constants, meaning that the actual detachment of the vesicles is slow. This means that they do not adhere but also do not go back to the bulk; that is, they remain close to the electrode. Although surprising at first sight, this observation is in agreement with what has been reported by Burgess et al. [49] who found that, although at certain potentials, the presence of an adsorbed bilayer on the surface of a gold electrode was not detectable by electrochemical measurements, its presence could still be detected by neutron reflectivity measurements, showing that the bilayer remained near to the electrode surface. Our experiments show that something similar happens with liposomes near a mercury electrode: they may not adhere and spread, but once they are close to the surface, they will not detach completely, or they will do so only very slowly.

Conclusions

Using high-resolution measurements with current sampling each 1.333 μs, the mechanism of adhesion and spreading of liposomes on a mercury electrode could be further elucidated. In previous reports [9, 10, 16–18], we have described the activation processes of the bilayer opening and rupture-spreading steps, the first one being the turning around of lecithin molecules and the second one being the formation of a pore large enough to disrupt the membrane. Both processes were shown to be related to certain properties of the membrane, such as the flip-flop rate and the rupture tension. In this publication, the kinetics of the previous step, interaction-docking, was elucidated, as the new measurements allow determining the time constant and activation energy of the process. It was found that the first interaction

Table 1 Dependence of the kinetic parameters of adhesion-spreading on the applied electrode potential (E) and the charge densities at the bare electrode surface (q_e)

E/V vs. Ag|AgCl	q_e^a/μC cm^{-2}	τ_0/μs	τ_1/μs	K_1	k_a/s^{-1}	k_b/s^{-1}	k_p/s^{-1}	k_a/k_b
−0.9	−9	11	110	1×10^4	1×10^5	1×10^8	0.5	1×10^{-3}
−0.6	−3.4	22	70	2×10^5	4×10^4	2×10^8	0.5	2×10^{-4}
−0.2	9.4	10	73	9×10^4	1×10^5	1.5×10^8	0.5	7×10^{-4}

[a] As reported by Hellberg et al. [10]

between the liposomes and the mercury surface is very weak, especially at low-charge densities, although the equilibrium condition is attained very quickly, and the high rate constant of the following step (bilayer opening) causes a displacement of the equilibrium, resulting in the adhesion-spreading of almost all of the liposomes reaching the electrode surface. The overall process is controlled by a mixed mechanism in which both, the kinetics of interaction-docking and the mass transport by diffusion, play an important role. The chronoamperometric measurements are shown to allow a detailed study of the complete adhesion-spreading process, from the liposomes in the bulk to the adsorbed lecithin island.

Acknowledgements V. A. H. acknowledges provision of a DAAD-Conacyt (Deutscher Akademischer Austauschdienst–Consejo Nacional de Ciencia y Tecnología, Germany–México) scholarship. F. S. acknowledges financial support by *Phospholipid Forschungszentrum e.V.* The authors gladly acknowledge provision of high-purity lecithin samples by Lipoid GmbH, Ludwigshafen, Germany.

Appendix 1

For the proposed mechanism:

$$\mathrm{L} \underset{k_p}{\overset{\text{Trans.}}{\rightleftarrows}} \mathrm{L'} \underset{k_b}{\overset{k_a}{\rightleftarrows}} \mathrm{L_D} \underset{\leftarrow}{\overset{K_1}{\rightarrow}} \mathrm{L_{D^*}} \xrightarrow{k_1} \mathrm{L_O} \underset{\leftarrow}{\overset{K_2}{\rightarrow}} \mathrm{L_{O^*}} \xrightarrow{k_2} \mathrm{L_E} \underset{\leftarrow}{\overset{K_3}{\rightarrow}} \mathrm{L_A}$$

the following system of differential equations describes the reaction:

- Reversible reaction, from the liposome L′ touching the electrode surface to the docked liposome L_D:

$$\frac{\mathrm{dL'}(t)}{\mathrm{d}t} = -k_\mathrm{a}\mathrm{L'}(t) + k_\mathrm{b}\mathrm{L_D}(t)$$

- Fast adsorption of the docked liposome followed by the bilayer opening:

$$\frac{\mathrm{dL_D}(t)}{\mathrm{d}t} = \frac{k_\mathrm{a}\mathrm{L'}(t) - k_\mathrm{b}\mathrm{L_D}(t) - k_1K_1\mathrm{L_D}(t)}{1+K_1}$$

- Fast adsorption of the opened liposome followed by the rupture-spreading:

$$\frac{\mathrm{dL_O}(t)}{\mathrm{d}t} = \frac{k_1K_1\mathrm{L_D}(t) - k_2K_2\mathrm{L_O}(t)}{1+K_2}$$

- Formation of the lecithin island and its adsorption:

$$\frac{\mathrm{dL_E}(t)}{\mathrm{d}t} = \frac{k_2K_2\mathrm{L_O}(t)}{1+K_3}$$

The set of differential equations is solved using Maple. The initial parameters consider a number L′0 of liposomes in contact with the electrode. The obtained constants defined as "_*C*#" are known and represent simplified forms of constants resulting from function of all rate constants. The results are:

$$\mathrm{L'}(t) = -\_C2 - \_C3 - \_C4 + \mathrm{L'}0 + \_C2\exp\left(\tfrac{k_2K_2}{1+K_2}t\right) + \_C3\%3 + \_C4\%2$$

$$\mathrm{L_O}(t) = \_C9 + \_C10\exp\left(\tfrac{k_2K_2}{1+K_2}t\right) + \_C11\%3 + (-\_C9 - \_C10 - \_C11)\%2$$

$$\mathrm{L_D}(t) = -\_C6 - \_C7 - \_C8 + \_C6\exp\left(\tfrac{k_2K_2}{1+K_2}t\right) + \_C7\%3 + \_C8\%2$$

$$\mathrm{L_E}(t) = \_C13 + (-\_C13 - \_C15 - \_C16)\exp\left(\tfrac{k_2K_2}{1+K_2}t\right) + \_C15\%3 + \_C16\%2$$

where:

$$\%2 = \exp\left(-\tfrac{1}{2}\tfrac{(k_a+k_aK_1+k_b+k_1K_1+\%1)t}{1+K_1}\right)$$
$$\%3 = \exp\left(-\tfrac{1}{2}\tfrac{(k_a+k_aK_1+k_b+k_1K_1-\%1)t}{1+K_1}\right)$$

and

$$\%1 = \sqrt{k_a^2 + 2k_a^2K_1 + 2k_ak_b - 2k_ak_1K_1 + k_a^2K_1^2 + 2k_ak_bK_1 - 2k_ak_1K_1^2 + k_b^2 + 2k_1k_bK_1 + k_1^2K_1^2}$$

Each of the intermediate products and the resulting lecithin islands produce a response (measured as charge). How much charge is displaced depends on how many lecithin molecules are involved in each of the intermediate steps and how they affect the double layer. Each of the intermediates then has a response assigned factor. The total charge displaced at any time will be given by the sum of all the responses.

$$Q_\mathrm{lip} = \text{factor 1} \times \mathrm{L'}(t) + \text{factor 2} \times \mathrm{L_D}(t) + \text{factor 3} \times K_1\mathrm{L_D}(t) + \text{factor 4} \times \mathrm{L_O}(t) + \text{factor 5} \times K_2\mathrm{L_O}(t) + \text{factor 6} \times \mathrm{L_E}(t) + \text{factor 7} \times K_3\mathrm{L_E}(t)$$

The constants multiplying each of the exponential terms (pre-exponential factors) can be extracted. Notice that the only all positive sum is present only by one of the constants, while the other two are predominantly negative. In fact, assigning values to the rate constants, two of the pre-exponential are negative, while a third (the one related with the bilayer opening process) is positive:

Coefficient for the exponential term %2 = $\exp\left(-\frac{1}{2}\frac{(k_a+k_aK_1+k_b+k_1K_1+\%1)t}{1+K_1}\right)$:

$$\begin{aligned}\text{constant 0} = {} & \text{factor 1\_}C4 - \text{factor 4\_}C11 \\ & - \text{factor 4\_}C10 + \text{factor 2\_}C8 \\ & + \text{factor 3 } K_1\text{\_}C8 - \text{factor 5 } K_2\text{\_}C9 \\ & - \text{factor 5 } K_2\text{\_}C10 - \text{factor 5 } K_2\text{\_}C11 \\ & - \text{factor 4 \_}C9 + \text{factor 6 \_}C16 \\ & + \text{factor 7 } K_3\text{\_}C16\end{aligned}$$

Coefficient for the exponential term %3 = $\exp\left(-\frac{1}{2}\frac{(k_a+k_aK_1+k_b+k_1K_1-\%1)t}{1+K_1}\right)$:

$$\begin{aligned}\text{constant 1} = {} & \text{factor } 3K_1\text{\_}C7 + \text{factor 4\_}C11 + \text{factor 1\_}C3 \\ & + \text{factor 2\_}C7 + \text{factor 6\_}C15 \\ & + \text{factor } 5K_2\text{\_}C11 + \text{factor } 7K_3\text{\_}C15\end{aligned}$$

Coefficient for the exponential term $\exp\left(\frac{k_2K_2}{1+K_2}t\right)$:

$$\begin{aligned}\text{constant 2} = {} & \text{factor 1\_}C2 - \text{factor } 7K_3\text{\_}C15 \\ & - \text{factor } 7K_3\text{\_}C13 + \text{factor } 3K_1\text{\_}C6 \\ & + \text{factor } 5K_2\text{\_}C10 + \text{factor 2\_}C6 \\ & - \text{factor } 7K_3\text{\_}C16 - \text{factor 6\_}C15 \\ & - \text{factor 6\_}C13 - \text{factor 6\_}C16 \\ & + \text{factor 4\_}C10\end{aligned}$$

An independent term $Y0$ is determined as the difference between the total displaced charge Q_{lip} and the above-determined coefficients multiplied by their correspondent exponential function:

$$\begin{aligned}Y0 = {} & -\text{factor } 3K_1\text{\_}C7 - \text{factor } 3K_1\text{\_}C8 \\ & - \text{factor } 3K_1\text{\_}C6 + \text{factor 6\_}C13 \\ & + \text{factor } 5K_2\text{\_}C9 + \text{factor } 7K_3\text{\_}C13 \\ & + \text{factor 4\_}C9 + \text{factor 2\_}C6 \\ & - \text{factor 2\_}C7 - \text{factor 2\_}C8 \\ & - \text{factor 1\_}C2 - \text{factor 1\_}C3 \\ & - \text{factor 1\_}C4 + \text{factor 1L'0}\end{aligned}$$

The Q_{lip} function can be then written as follows:

$$\begin{aligned}Q_{lip} = {} & Y0 + \text{constant } 0 \times \%2 + \text{constant } 1 \times \%3 \\ & + \text{constant } 2 \times \exp\left(\frac{k_2K_2}{1+K_2}t\right)\end{aligned}$$

This function can be rewritten as:

$$\begin{aligned}Q_{lip} = {} & Y0 + \text{constant } 0 + \text{constant } 1 + \text{constant } 2 \\ & - \text{constant } 0 \times (1 - \%2) - \text{constant } 1 \times (1 - \%3) \\ & - \text{constant } 2 \times \left(1 - \exp\left(\frac{k_2K_2}{1+K_2}t\right)\right)\end{aligned}$$

According to the empirical equation used to fit the experimental curves, it follows that:

Q_0 =−constant 0 (positive)
Q_1 =−constant 1 (negative)
Q_2 =−constant 2 (positive)

Notice that Q_1 is negative even though all factors are considered positive! The negative value arises to account for the consumption of the intermediate states and is compensated by the formation of the final product (the lecithin island). The actual charge difference at the electrode, at any time is positive, and the charge flowing as a result of any process of formation is also positive!

An independent term will be equal to: $Y0$+constant 0+constant 1+constant 2:

$$\text{independent} = \text{factor } 1 \times \text{L'}(0)$$

As L′ represents the liposome after instant contact with the electrode, before interaction docking and, therefore, without charge displacement, factor 1=0, and there is no independent constant term in the equation. With the appropriate substitutions, Eqs. 2 and 4 are obtained:

$$\begin{aligned}Q_{lip} = {} & Q_0\left(1 - e^{-\frac{t}{\frac{2(1+K_1)}{(Z+Y)}}}\right) + Q_1\left(1 - e^{-\frac{t}{\frac{2(1+K_1)}{(Z-Y)}}}\right) \\ & + Q_2\left(1 - e^{-\frac{t}{\frac{(1+K_2)}{(k_2K_2)}}}\right)\end{aligned}$$

and

$$Q_{lip} = Q_0\left(1 - e^{-\frac{t}{\tau_0}}\right) + Q_1\left(1 - e^{-\frac{t}{\tau_1}}\right) + Q_2\left(1 - e^{-\frac{t}{\tau_2}}\right)$$

Appendix 2

Defining the rate of formation and consumption of vesicles at the electrode surface (L′(t)): Transport mechanism by

diffusion, reversible interaction docking, and a term $k_p \times L'(t)$ representing a simplified form of the diffusion of nonreactant vesicles from the surface to the bulk:

$$\frac{dL'(t)}{dt} = \frac{C_{lip} A_{SMDE} \sqrt{D}}{\sqrt{\pi}\sqrt{t}} - k_a L'(t) + k_b L'(t) - k_p L'(t)$$

The reaction is followed by a reversible interaction docking which is then followed by an irreversible reaction:

$$\frac{dL_D(t)}{dt} = k_a L'(t) - k_b L_D(t) - k_n L_D(t)$$

After the irreversible reaction with the rate constant k_n, there is no other possibility for the vesicle than to rupture and produce a response peak, and therefore, the rate of formation of peaks is defined as:

$$\frac{dN(t)}{dt} = k_n L_D(t)$$

Applying the initial condition $L'(0)=0$, the differential equations are simultaneously solved, and the number of peaks as a function of time results in the function:

$$N(t) = \frac{-16\sqrt{D} A_{SMDE} C_{lip} k_a k_n}{\sqrt{\pi}\%5\%4\%1\%3^2\%2^2} \begin{pmatrix} -2k_p k_n \sqrt{\%1\%5\%4 t} - 2k_p k_b \sqrt{\%1\%5\%4 t} \\ -2k_a k_n \sqrt{\%1\%5\%4 t} - 2k_p k_b k_n \sqrt{\pi}\%4\%6 \times \exp\left(-\frac{1}{2}\%3 t\right) \\ -k_p^2 k_n \sqrt{\pi}\%4\%6 \times \exp\left(-\frac{1}{2}\%3 t\right) + k_p^2 k_n \sqrt{\pi}\%5\%7 \times \exp\left(-\frac{1}{2}\%2 t\right) \\ +k_p k_a k_b \sqrt{\pi}\%5\%7 \times \exp\left(-\frac{1}{2}\%2 t\right) + k_n k_a k_b \sqrt{\pi}\%5\%7 \times \exp\left(-\frac{1}{2}\%2 t\right) \\ -k_p k_b k_a \sqrt{\pi}\%4\%6 \times \exp\left(-\frac{1}{2}\%3 t\right) - k_n^2 k_a \sqrt{\pi}\%4\%6 \times \exp\left(-\frac{1}{2}\%3 t\right) \\ -k_n k_b k_a \sqrt{\pi}\%4\%6 \times \exp\left(-\frac{1}{2}\%3 t\right) - k_n^2 k_p \sqrt{\pi}\%4\%6 \times \exp\left(-\frac{1}{2}\%3 t\right) \\ +k_n^2 k_p \sqrt{\pi}\%5\%7 \times \exp\left(-\frac{1}{2}\%2 t\right) - k_p^2 k_n \sqrt{\pi}\%4\%6 \times \exp\left(-\frac{1}{2}\%3 t\right) \\ +2k_p k_n k_b \sqrt{\pi}\%5\%7 \times \exp\left(-\frac{1}{2}\%2 t\right) + k_b^2 k_p \sqrt{\pi}\%5\%7 \times \exp\left(-\frac{1}{2}\%2 t\right) \\ -k_n k_p k_a \sqrt{\pi}\%4\%6 \times \exp\left(-\frac{1}{2}\%3 t\right) + k_p^2 k_b \sqrt{\pi}\%5\%7 \times \exp\left(-\frac{1}{2}\%2 t\right) \\ +k_p k_n \sqrt{\pi}\%1\%5\%7 \times \exp\left(-\frac{1}{2}\%2 t\right) + k_p k_b \sqrt{\pi}\%1\%4\%6 \times \exp\left(-\frac{1}{2}\%3 t\right) \\ +k_a k_n \sqrt{\pi}\%1\%4\%6 \times \exp\left(-\frac{1}{2}\%3 t\right) + 2k_p k_n k_a \sqrt{\pi}\%5\%7 \times \exp\left(-\frac{1}{2}\%2 t\right) \\ +k_p k_b \sqrt{\pi}\%1\%5\%7 \times \exp\left(-\frac{1}{2}\%2 t\right) + k_a k_n \sqrt{\pi}\%1\%5\%7 \times \exp\left(-\frac{1}{2}\%2 t\right) \\ -k_b^2 k_p \sqrt{\pi}\%4\%6 \times \exp\left(-\frac{1}{2}\%3 t\right) + k_a^2 k_n \sqrt{\pi}\%5\%7 \times \exp\left(-\frac{1}{2}\%2 t\right) \\ +k_n^2 k_a \sqrt{\pi}\%5\%7 \times \exp\left(-\frac{1}{2}\%2 t\right) + k_p k_n \sqrt{\pi}\%1\%4\%6 \times \exp\left(-\frac{1}{2}\%3 t\right) \\ -k_a^2 k_n \sqrt{\pi}\%4\%6 \times \exp\left(-\frac{1}{2}\%3 t\right) \end{pmatrix}$$

where

$$\begin{aligned} \%1 &= k_a^2 + 2k_a k_p + 2k_a k_b - 2k_a k_n + k_p^2 \\ &\quad -2k_p k_b - 2k_p k_n + k_b^2 + 2k_n k_b + k_n^2 \\ \%2 &= k_a + k_p + k_b + k_n - \sqrt{\%1} \\ \%3 &= k_a + k_p + k_b + k_n + \sqrt{\%1} \\ \%4 &= -2 \times \%2 \\ \%5 &= -2 \times \%3 \\ \%6 &= \mathrm{erf}\left(\tfrac{1}{2}\sqrt{\%5 t}\right) \\ \%7 &= \mathrm{erf}\left(\tfrac{1}{2}\sqrt{\%4 t}\right) \end{aligned}$$

The equation thus obtained can be simplified to:

$$\begin{aligned} N(t) = {} & \frac{Z_o \mathrm{erf}\left(\frac{1}{2}\sqrt{t}\sqrt{-2(Y_o + X_o)}\right)}{X_o (Y_o - X_o)(Y_o + X_o)^2 \sqrt{-2(Y_o + X_o)}} \\ & \times \exp\left(-\frac{1}{2}(Y_o + X_o)t\right) \\ & - \frac{Z_o \mathrm{erf}\left(\frac{1}{2}\sqrt{t}\sqrt{-2(Y_o - X_o)}\right)}{X_o (Y_o - X_o)^2 (Y_o + X_o) \sqrt{-2(Y_o - X_o)}} \\ & \times \exp\left(-\frac{1}{2}(Y_o - X_o)t\right) \\ & + \frac{2Z_o \sqrt{t}}{\sqrt{\pi}(Y_o - X_o)^2 (Y_o + X_o)^2} \end{aligned}$$

where:

$$X_o = \sqrt{k_a^2 + 2k_ak_p + 2k_ak_b - 2k_ak_n + k_p^2 - 2k_pk_b - 2k_pk_n + k_b^2 + 2k_nk_b + k_n^2}$$
$$Y_o = k_a + k_p + k_b + k_n$$
$$Z_o = 16A_{SMDE}C_{lip}^{*}\sqrt{D}k_ak_n\left(k_ak_n + k_pk_b + k_pk_n\right)$$

Grouping all constant terms, the equation is further simplified to:

$$N(t) = A_{SMDE}C_{lip}^{*}\sqrt{D}\left(A_1\mathrm{erf}\left(\sqrt{-k_{o1}t}\right)e^{-k_{o1}t} + A_2\mathrm{erf}\left(\sqrt{-k_{o2}t}\right)e^{-k_{o2}t} + A_3\sqrt{t}\right)$$

corresponding to Eq. 11.

References

1. Lasic DD (1992) Am Sci 80:20
2. Lasic DD (1995) Applications of liposomes. In: Lipowski R, Sackmann E (eds) Structure and dynamics of membranes. From cells to vesicles. Elsevier, Holland
3. Terzano C, Allegra L, Alhaique F, Marianecci C, Carafa M (2005) Eur J Pharm Biopharm 59:57. doi:10.1016/j.ejpb.2004.06.010
4. Carafa M, Di Marzio L, Marianecci C, Cinque B, Lucania K, Kajiwara K, Cifone MG, Santucci E (2006) Eur J Pharm Sci 28:385. doi:10.1016/j.ejps.2006.04.009
5. Johansson E, Engvall C, Arfvidsson M, Lundahl P, Edwards K (2005) Biophys Chem 113:183. doi:10.1016/j.bpc.2004.09.006
6. Katragadda A, Bridgman R, Betageri G (2000) Cell Mol Biol Lett 5:483
7. Semple SC, Leone R, Wang J, Leng EC, Klimuk SK, Eisenhardt ML, Yuan Z, Edwards K, Maurer N, Hope MJ, Cullis PR, Ahkong Q (2005) J Pharm Sci 94:1024. doi:10.1002/jps.20332
8. Zhigaltsev IV, Maurer N, Edwards K, Karlsson G, Cullis PR (2006) J Control Release 110:378. doi:10.1016/j.jconrel.2005.10.011
9. Hellberg D, Scholz F, Schauer F, Weitschies W (2002) Electrochem Commun 4:305. doi:10.1016/S1388-2481(02)00279-5
10. Hellberg D, Scholz F, Schubert F, Lovrić M, Omanović D, Agmo Hernández V, Thede R (2005) J Phys Chem B 109:14715. doi:10.1021/jp050816s
11. Miller IR, Rishpon J, Tenenbaum A (1976) Bioelectrochem Bioenerg 3:528. doi:10.1016/0302-4598(76)80043-8
12. Nelson A, Auffret N (1988) J Electroanal Chem 244:99. doi:10.1016/0022-0728(88)80098-6
13. Leermarkers FAM, Nelson A (1990) J Electroanal Chem 278:53. doi:10.1016/0022-0728(90)85123-M
14. Nelson A, Leermarkers FAM (1990) J Electroanal Chem 278:73. doi:10.1016/0022-0728(90)85124-N
15. Bizzotto D, Yang Y, Shepherd JL, Stoodley R, Agak J, Stauffer V, Lathuillière M, Akhtar AS, Chung E (2004) J Electroanal Chem 574:167. doi:10.1016/j.jelechem. 2003.11.002
16. Agmo Hernández V, Scholz F (2006) Langmuir 22:10723. doi:10.1021/la060908o
17. Agmo Hernández V, Scholz F (2008) Bioelectrochemistry (in press). doi:10.1016/j.bioelechem.2008.06.007
18. Agmo Hernández V, Scholz F (2008) Isr J Chem (in press)
19. Press WH, Flannery BP, Teukolsky SA, Vetterling WT (1992) Numerical recipes in Pascal. Cambridge University Press, Cambridge, MA
20. Lee J, Lentz BR (1998) Proc Natl Acad Sci USA 95:9274. doi:10.1073/pnas.95.16.9274
21. Zimmerberg J, Chernomordik LV (1999) Adv Drug Deliv Rev 38:197. doi:10.1016/S0169-409X(99)00029-0
22. Chanturiya A, Scaria P, Kuksenok O, Woodle MC (2002) Biophys J 82:3072
23. Chizmadzhev YA, Kuzmin PI, Kumenko DA, Zimmerberg J, Cohen FS (2000) Biophys J 78:2241
24. Heuvingh J, Pincet F, Cribier S (2004) Eur Phys J E 14:269. doi:10.1140/epje/i2003-10151-2
25. Kozlovsky Y, Chernomordik LV, Kozlov MM (2002) Biophys J 83:2634
26. Monck JR, Fernandez JM (1992) J Cell Biol 119:1395. doi:10.1083/jcb.119.6.1395
27. Žutić V, Svetličić V, Zimmerman AH, DeNardis NI, Frkanec R (2007) Langmuir 23:8647. doi:10.1021/la063712x
28. Agmo Hernández V, Scholz F (2007) Langmuir 23:8650. doi:10.1021/la7009435
29. Maisonhaute E, White PC, Compton RG (2001) J Phys Chem B 105:12087. doi:10.1021/jp012437e
30. Maisonhaute E, Brookes BA, Compton RG (2002) J Phys Chem B 106:3166. doi:10.1021/jp013448a
31. Banks CE, Rees NV, Compton RG (2002) J Phys Chem B 106:5810. doi:10.1021/jp020696d
32. Rees NV, Banks CE, Compton RG (2004) J Phys Chem B 108:18391. doi:10.1021/jp040602v
33. Davies TJ, Lowe ER, Wilkins SJ, Compton RG (2005) ChemPhysChem 6:1340. doi:10.1002/cphc.200500152
34. Fietkau N, Du G, Matthews SM, Johns ML, Fisher AC, Compton RG (2007) J Phys Chem C 111:7801. doi:10.1021/jp070429d
35. Omanović D. Signal Counter. Rudjer Boskovic Institute, Zagreb, Croatia (E-mail: omanovic@irb.hr)
36. Moscho A, Orwar O, Chiu DT, Modi BP, Zare RN (1996) Proc Natl Acad Sci USA 93:11443. doi:10.1073/pnas.93.21.11443
37. Berndl K, Käs J, Lipowsky R, Sackmann E (1990) Europhys Lett 13:659. doi:10.1209/0295-5075/13/7/015
38. Sackmann E (1994) FEBS Lett 346:3. doi:10.1016/0014-5793(94)00484-6
39. Tsekov R, Kovač S, Žutić V (1999) Langmuir 15:5649. doi:10.1021/la980944q
40. Milchev A (2002) Electrocrystallization. Fundamentals of nucleation and growth. Kluwer, Boston, MA
41. Milchev A (2008) Russ J Electrochem 44:619. doi:10.1134/S1023193508060025
42. Dausheva MR, Songina OA (1973) Russ Chem Rev 42:136. doi:10.1070/RC1973v042n02ABEH002570
43. Evans E, Rawicz W (1990) Phys Rev Lett 64:2094. doi:10.1103/PhysRevLett.64.2094
44. Sackmann E (1995) Physical basis of self-organization and function of membranes: physics of vesicles. In: Lipowski R, Sackmann E (eds) Structure and dynamics of membranes. From cells to vesicles. Elsevier, Holland
45. Lipowski R (1998) In: Trigg GL (ed) Encyclopedia of applied physics. vol. 23. Wiley, New York
46. Miller IR (1981) Charge transport in lipid layers and in biological membranes. In: Milazzo G (ed) Topics in bioelectrochemistry and bioenergetics. Wiley, Chichester
47. Nelson A, Benton A (1986) J Electroanal Chem 202:253. doi:10.1016/0022-0728(86)90123-3
48. Moncelli MR, Becucci L, Guidelli R (1994) Biophys J 66:1969
49. Burgess I, Li M, Horswell SL, Szymanski G, Lipkowski J, Majewski J, Satija S (2004) Biophys J 86:1763